




## Article

# Impact of redox evolution of layered double hydroxides on the immobilisation of structural and adsorbed heavy metals

Mengyao Yuan, Minwang Laipan , Min Zhang, Xueya Wan, Ziyu Wang and Junkang Guo

School of Environmental Science and Engineering, Shaanxi University of Science and Technology, Xi'an, 710021, China

### Abstract

In the soil environment, divalent heavy metal ions often interact with trivalent metal ions to form hydrotalcite supergroup nanominerals (also known as natural layered double hydroxides, LDHs), effectively immobilising heavy metals within the minerals structure. Concurrently, these LDH minerals also show high surface reactivity and can adsorb surrounding heavy metal ions, thus they play a significant role in heavy metal pollution purification. However, the impact of the subsequent geochemical evolution of heavy-metal-containing LDHs on the migration and transformation of structural and surface-adsorbed heavy metals as well as its surface reactivity towards surrounding heavy metals remains unclear. Herein, Ni(II)Fe(III)-LDH and Co(II)Al(III)-LDH were taken as examples to reveal the influence of redox evolution on the immobilisation of structural and adsorbed heavy metals. The results of this work indicate that the oxidative–reductive alternating evolution of structural Ni, Fe and Co elements constrain the transformation of heavy metals, as well as their bioavailability greatly. The oxidative–reductive alternating evolution helped reduce the content of bioavailable heavy metals in exchangeable and carbonate-bounded states. It can also enhance the integration of heavy metals with the LDH structure and help transform heavy metals into residual states, thereby reducing their mobility and bioavailability. However, oxidative–reductive evolution significantly reduced the surface reactivity of LDHs, diminishing their interface locking ability for surrounding heavy metal ions. This research provides foundational data for assessing the long-term environmental performance of LDHs.

**Keywords:** layered double hydroxides; heavy metals; nanominerals; geochemical evolution; migration and transformation

(Received 29 May 2024; accepted 4 August 2024; Accepted Manuscript published online: 11 November 2024)

### Introduction

With the rapid development of industrialisation and urbanisation, soil heavy metal pollution has become an increasingly prominent environmental issue (Liu *et al.*, 2022, Qiu *et al.*, 2022). In China, nearly 20 million hectares of farmland are affected by heavy metals, accounting for about one-fifth of the total arable land (Sodango *et al.*, 2018). Addressing soil heavy metal pollution has become an urgent problem, and varied methods have been developed for heavy metals immobilisation and extraction, including adsorption (Muhammad *et al.*, 2021, Haris *et al.*, 2022, Zhang *et al.*, 2022), precipitation (Zhou *et al.*, 2010, Xu *et al.*, 2023), ion exchange (Guo *et al.*, 2021, Qiu *et al.*, 2022), solvent extraction (de Souza E Silva *et al.*, 2006), membrane separation (Ahmad *et al.*, 2022), electrochemical means (Wang *et al.*, 2022a) and biological approaches (Guo *et al.*, 2020, Liu *et al.*, 2024). It's believed that soil minerals play a unique role in controlling pollution, as they can adsorb and immobilise heavy metal ions (Zhu *et al.*, 2016, Wang *et al.*, 2022b,

Liu *et al.*, 2024); more importantly, some minerals can lock heavy metals within their lattice, effectively reducing the mobility and bioavailability of heavy metal ions (Siebecker *et al.*, 2018, Laipan *et al.*, 2024). Heavy metal ions may engage in the mineral formation process once they enter the soil; therefore, studies with a particular emphasis on the interaction between soil mineral particles or free metal ions and heavy metal ions have become the focus of research (Siebecker *et al.*, 2018).

In recent years, the interaction of divalent heavy metal ions with metal oxides or clay minerals in soil to form layered double hydroxide supergroup nanominerals has emerged as a new hot topic (Siebecker *et al.*, 2018). Layered double hydroxides (LDHs), including hydrotalcite and hydrotalcite-like minerals, are primarily composed of divalent and trivalent metal hydroxides (Yu *et al.*, 2017, Laipan *et al.*, 2020). The main reason for the interest in LDH supergroup minerals in soil is that divalent heavy metal ions can readily form LDH minerals with widely present  $\text{Al}^{3+}/\text{Fe}^{3+}$  or  $\text{Al}^{3+}/\text{Fe}^{3+}$ -containing soil minerals in aqueous media, achieving the fixation of heavy metals within the LDH lattice (Peltier *et al.*, 2010, Zhu and Elzinga 2014, Aucour *et al.*, 2015, Laipan *et al.*, 2024). Concurrently, the high surface reactivity of LDH nanominerals plays a significant role in the adsorption of heavy metals (Liang *et al.*, 2013, He *et al.*, 2018, Laipan *et al.*, 2023). Thus, LDHs play a critical role in heavy metal immobilisation both by adsorption and lattice fixation in the soil environment.

**Corresponding author:** Minwang Laipan; Email: [laipanminwang@sust.edu.cn](mailto:laipanminwang@sust.edu.cn)

**Associate Editor:** Runliang Zhu

This paper is part of a thematic set on Nanominerals and mineral nanoparticles

**Cite this article:** Yuan M, Laipan M, Zhang M, Wan X, Wang Z and Guo J (2025). Impact of redox evolution of layered double hydroxides on the immobilisation of structural and adsorbed heavy metals. *Mineralogical Magazine*, 1–9. <https://doi.org/10.1180/mgm.2024.61>

However one concern here is whether LDHs can immobilise surface adsorbed and lattice-fixed heavy metals chronically or permanently. This will depend on the variation of LDH stability and surface reactivity during the long-term geochemical evolution in the soil environment. Due to the complexity of the soil environment, the geochemical evolution processes of LDHs occur inevitably. Natural LDHs, especially those heavy-metal-bearing LDHs mostly contain metal elements (e.g. Cu, Co, Ni and Fe) that can be reduced or oxidised in the environment by reducing and oxidising substances/species (such as reducing organic matter, photo-generated electrons/holes, surface active oxygen species, etc.) (Laipan *et al.*, 2020). Therefore, it is likely that heavy-metal-bearing LDHs may undergo alternating oxidation and reduction evolution processes. However, there is insufficient understanding of the variation of stability and surface reactivity of heavy-metal-bearing LDH minerals during subsequent geochemical evolution processes in the soil environment, as well as the potential re-migration and transformation behaviours of heavy metals in these minerals.

To examine the impact of oxidation–reduction alternating evolution on the structural stability, surface reactivity, heavy metal locking performance, and heavy metal re-migration and transformation behaviours of heavy-metal-bearing LDHs, CoAl-LDH and NiFe-LDH were used as representatives. By repeatedly altering the valence states of structural Co and Fe in a LDH, this study investigated how the redox evolution affects the structure of a LDH, the state of heavy metal existence, the migration and transformation of heavy metals, and the variation in adsorption performance of LDHs with heavy metal species. The findings provide experimental evidence for assessing the long-term performance of LDHs in heavy metal immobilisation.

## Materials and methods

### Synthesis of LDHs

Using metal nitrates as starting materials, CoAl-LDH and NiFe-LDH, containing divalent heavy metal ions Co(II) and Ni(II), respectively, were synthesised through conventional coprecipitation methods (Laipan *et al.*, 2023, Laipan *et al.*, 2024), with a molar ratio of divalent to trivalent ions of 2:1. For CoAl-LDH synthesis, a 500 mL solution of  $\text{Co}(\text{NO}_3)_2 \cdot 6\text{H}_2\text{O}$  (0.1 mol/L) and  $\text{Al}(\text{NO}_3)_3 \cdot 9\text{H}_2\text{O}$  (0.05 mol/L) and a 500 mL base solution containing 0.5 mol/L NaOH and 0.1 mol/L  $\text{Na}_2\text{CO}_3$  were first prepared. These solutions were then simultaneously added dropwise to a 2 L beaker (initially containing 200 mL of ultrapure water) using an automatic pH dosing machine (Kroma CPH-2). The reaction was conducted under continuous magnetic stirring and a pH of  $8 \pm 0.1$ . Subsequently, the mixture was stirred for an additional 2 hours and then left to age for 12 hours. Following ageing, the solid was collected by centrifuging and washed with ultrapure water until the supernatant reached near-neutral pH. Then the product was separated and dried to obtain the CoAl-LDH. The synthesis of NiFe-LDH was using the same procedures, but using  $\text{Ni}(\text{NO}_3)_2 \cdot 6\text{H}_2\text{O}$  and  $\text{Fe}(\text{NO}_3)_3 \cdot 9\text{H}_2\text{O}$  to replace  $\text{Co}(\text{NO}_3)_2 \cdot 6\text{H}_2\text{O}$  and  $\text{Al}(\text{NO}_3)_3 \cdot 9\text{H}_2\text{O}$ , respectively.

### Alternating oxidation and reduction of LDHs

Sodium borohydride and hydrogen peroxide were selected to carry out the oxidation–reduction reaction on CoAl-LDH and

NiFe-LDH. For CoAl-LDH, a certain amount of CoAl-LDH was placed in a beaker, and hydrogen peroxide solution (mass ratio of 30%) was added in the beaker with a ratio of 1 g LDH per 20 mL of hydrogen peroxide solution. The reaction was stirred for 30 minutes to oxidise the divalent cobalt ions in CoAl-LDH. After oxidation, the product was washed with ultrapure water and dried. The resulting product is the first oxidation product of CoAl-LDH; the product hereafter is named as CoAl-LDH-FO (FO: first oxidised). After that, CoAl-LDH-FO was reduced by sodium hydroxide to generate the first reduction product, CoAl-LDH-FR. The procedure is as follows: an amount of the CoAl-LDH-FO was put into a beaker which contains sodium hydroxide solution (pH 10) with a solid–liquid ratio of 1 g : 20 mL. Then, borohydride sodium was added into the beaker with a ratio of 1 g LDH to 100 mg of borohydride sodium, and the solution was stirred for 30 minutes to reduce the metal ions of Co(III). After reduction, the product (CoAl-LDH-FR) was washed three times with ultrapure water and dried. This was repeated, alternating oxidation and reduction processes, to obtain the second oxidised and second reduced products CoAl-LDH-SO and CoAl-LDH-SR. In summary, the original CoAl-LDH underwent the stages: first oxidation – first reduction – second oxidation – second reduction.

The oxidation–reduction evolution of NiFe-LDH is similar to the above process, with the difference being the reduction reaction happened first and was followed by the oxidation reaction. That is, NiFe-LDH underwent: first reduction – first oxidation – second reduction – second oxidation, which generated the products: NiFe-LDH-FR, NiFe-LDH-FO, NiFe-LDH-SR and NiFe-LDH-SO.

To reveal any leaching of heavy metals from LDHs during the REDOX process, concentrations of the heavy metals in the solution generated from each evolution process as well as the heavy metal contents in the original LDH were determined by ICP-MS (7900, Agilent).

### Determination of ratio of Co(II)/Co(III) and Fe(II)/Fe(III)

Co(II)/Co(III) and Fe(II)/Fe(III) ratios were determined after each oxidation or reduction process. All the CoAl-LDH and NiFe-LDH were dissolved by HCl to obtain Co and Fe solution. Then, Co(II) detection was conducted using a Nitroso-R salt spectrophotometric method (Yu *et al.*, 2024). In detail, in sodium acetate (pH 5.5–6.0) solution, Co(II) ions can react with nitroso-R salt (also known as NRS) to form soluble red complexes; the concentration of these red complexes can be determined at 530 nm by using a UV/VIS spectrophotometer. The concentration of Fe(II) was detected by the 1,10-phenanthroline method (Liang *et al.*, 2019). The total amounts of Co and Fe in the LDH were detected by ICP-MS as stated above. Finally, the ratios of Co(II)/Co(III) and Fe(II)/Fe(III) can be obtained via above procedures.

### Testing of metal occurrence forms in LDHs

Metals (Ni, Fe, Co and Al) in the original, oxidised, and reduced LDH were extracted using the Tessier method to determine their occurrence forms (Tessier *et al.*, 1979). First step: 2 g of each LDH was put in a 25 mL centrifuge tube, and then 16 mL of 1 mol/L  $\text{MgCl}_2$  (pH=7) was added into the tube. The reaction lasted for 1 hour at room temperature under oscillation. After oscillation, the samples were centrifuged at 4000 rpm for 10 minutes, and the supernatant was collected for a heavy metal concentration test and the solid was used for the following experiments. Second step: 16 mL of 1 mol/L NaAc (pH = 5.5, adjusted by HAc) was added

into the tube which contained the residual solid of the first step. The reaction lasted for 5 hours at room temperature under oscillation. After oscillation, the samples were centrifuged for 10 minutes. The supernatant was collected for a heavy-metal concentration test and the solid was used for the third step. Third step: the resulting solid from the second step was dried and digested, and the heavy-metal concentration was measured using ICP-MS after dilution. Each experiment was repeated twice. As this LDH does not contain organic matter and iron-manganese oxides, we mainly determined exchangeable, carbonate bounded and residual forms of metals.

### Cd adsorption experiment

The adsorption of  $\text{Cd}^{2+}$  was used to evaluate the effect of alternating oxidation–reduction evolution on the surface adsorption reactivity of LDHs, and further to estimate whether oxidation–reduction evolution would cause the re-migration of surface-adsorbed heavy metals on LDHs. Batch adsorption experiments were conducted to determine the isothermal adsorption behaviour. The adsorption experiments were carried out in a covered glass tube, with an adsorbent addition of 1 g/L. The  $\text{Cd}^{2+}$  concentration ranging from 5–100 mg/L. The reactions were conducted for 12 hours under pH of 7, 25°C, and oscillation. After adsorption, the samples were centrifuged, and the  $\text{Cd}^{2+}$  concentration in the supernatant was measured by ICP-MS.

### Characterisation methods

X-ray diffraction analysis (XRD) of the products were measured on a Bruker D8 ADVANCE X-ray diffractometer using  $\text{CuK}\alpha$  radiation operating at 40 kV and 40 mA. The patterns were recorded over the  $2\theta$  range from 3 to 80° with a scan speed of 3°/min using a bracket sample holder. XRD primarily served to determine whether the LDH structure was destroyed after the redox reaction. Images were obtained using a Gemini SEM 460 (ZEISS) high-resolution field emission scanning electron microscope (SEM). A zeta potential test was used primarily to measure the charge state of the LDH. Variation of the Zeta potential with pH of the products was detected by Malvern Zetasizer Nano-ZS (Malvern Instruments, UK). 1 mmol/L  $\text{NaNO}_3$  was used as electrolyte solution during the measurements (Liu *et al.*, 2018), and all the measurements were accomplished at room temperature.

## Results and discussion

### Effects of redox evolution on the structural and surface characteristics of LDHs

The XRD results show that there is no significant phase change between the original CoAl-LDH and its first oxidised sample (CoAl-LDH-FO), but the  $d(003)$  value of the CoAl-LDH-FO (0.871 nm) is reduced by ca. 0.02 nm compared with that of the original CoAl-LDH (0.890 nm) (Fig. 1a). This is because the structural Co(II) (ionic radius 74.5 pm) is oxidised to Co(III) (ionic radius 54.5 pm); the reduction of ionic radius caused a shift to a higher diffraction angle (Deng *et al.*, 2018). The subsequent redox reaction would completely destroy the LDH structure resulting in the formation of amorphous products (CoAl-LDH-FR, CoAl-LDH-SO and CoAl-LDH-SR) indicated by the disappearance of all diffraction peaks. Guo *et al.* also indicated that the oxidation

of  $\text{Co}^{2+}$  to  $\text{Co}^{3+}$  in NiCo-LDH would result in the disappearance of the characteristic diffraction peaks of the layered structure (Gou *et al.*, 2016). Therefore, the disappearance of characteristic diffraction peaks of the LDH herein should be due to the change of valence state of Co. As for NiFe-LDH, XRD results indicate that there is no significant phase change before and after oxidative–reductive alternating evolution, but that the oxidative–reductive alternating evolution affected the layer stacking of LDH nano plates on the c-axis (Fig. 1b).

Zeta potential test results showed that original LDH and the oxidised and reduced products all have a positively charged surface (Fig. 2), indicating that the sample may still retain part of the LDH structure after oxidation and reduction. As the amount of positive charge of the LDH is dependent on the content of structural metal in a higher valence state, destruction of the layered structure of a LDH would alter the content of structural metals and thus change the surface charge of the LDH (Laipan *et al.*, 2020). For CoAl-LDH, after the first oxidation, the surface charge in pH 7–10 (from 26–24 mV) is higher than the original one (from 25.2–22.5 mV), indicating that oxidation will not destroy the LDH structure, in good agreement with the XRD results. The reason for the increase of the charge may be that the first oxidation promotes the integrity of the LDH structure (Fig. 1a). However, the subsequent reduction and oxidation significantly reduced the surface charge of the products (decrease from 28–18 mV to 3–0.5 mV in the pH range of 5–11), indicating that the subsequent treatment will significantly destroy the structure of the LDH, which is consistent with the XRD results.

Regarding NiFe-LDH, the zeta potential test results demonstrated that the oxidative–reductive evolution also has a significant impact on the structure of NiFe-LDH. But unlike CoAl-LDH, the oxidation and reduction led to an increase of the positive charge of NiFe-LDH (mostly increases from 1.5–0.6 mV to 3.25–0.75 mV in pH range of 5–11, Fig. 2b), indicating that the reduced and oxidised products of NiFe-LDH may retain the LDH structure after multiple oxidative–reductive treatments, in agreement with the XRD results. The increase in positive charge content also indicates that there are certain changes in the proportion and occupancy of Ni and Fe in the structural layers of NiFe-LDH, possibly due to the detachment of some Ni(II) from the structural layers of the LDH during the oxidative–reductive evolution (See Fig. 4b later), leading to a higher proportion of  $\text{Fe}^{3+}$  in the products compared to the original sample. This inference is based on the fact that the amount of structural charge of a LDH depends mainly on the content of the structural metal element with higher oxidation state (Yu *et al.*, 2017; Laipan *et al.*, 2020). Additionally, previous studies also indicated that  $\text{Ni}^{2+}$  can be oxidised to  $\text{Ni}^{3+}$  (Zhao *et al.*, 2015; Liu *et al.*, 2017), thus the amount of positive charge on the LDH layers has increased.

Scanning electron microscopy images also suggest the destruction or preservation of the LDH structure of the reduced and oxidised LDH (Fig. 3). For CoAl-LDH, the sheet-like morphology has been destroyed markedly by redox evolution, and the sheets have been transferred to dense blocks as redox evolution progresses. This result indicates the destruction of the CoAl-LDH structure, in good agreement with XRD results. As also indicated by the XRD results, CoAl-LDH-FO and CoAl-LDH showed similar diffraction peaks with comparable diffraction intensity; therefore CoAl-LDH-FO should have similar morphology with CoAl-LDH. The SEM image of CoAl-LDH-FO in Fig. 3 fits well with the above reasoning. As reduction and oxidation proceed, the sheets were transferred to dense blocks. Regarding NiFe-LDH, the redox

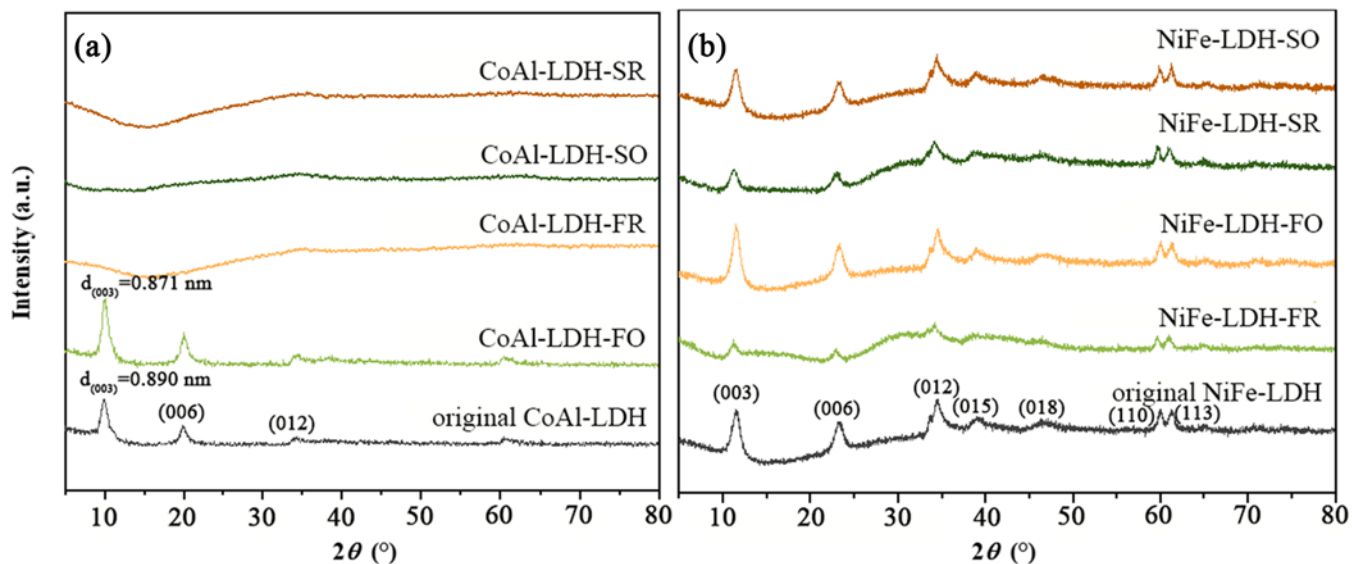


**Figure 1.** XRD patterns of the original, oxidised and reduced LDHs: (a) CoAl-LDH and its oxidised and reduced products; (b) NiFe-LDH and its oxidised and reduced products.

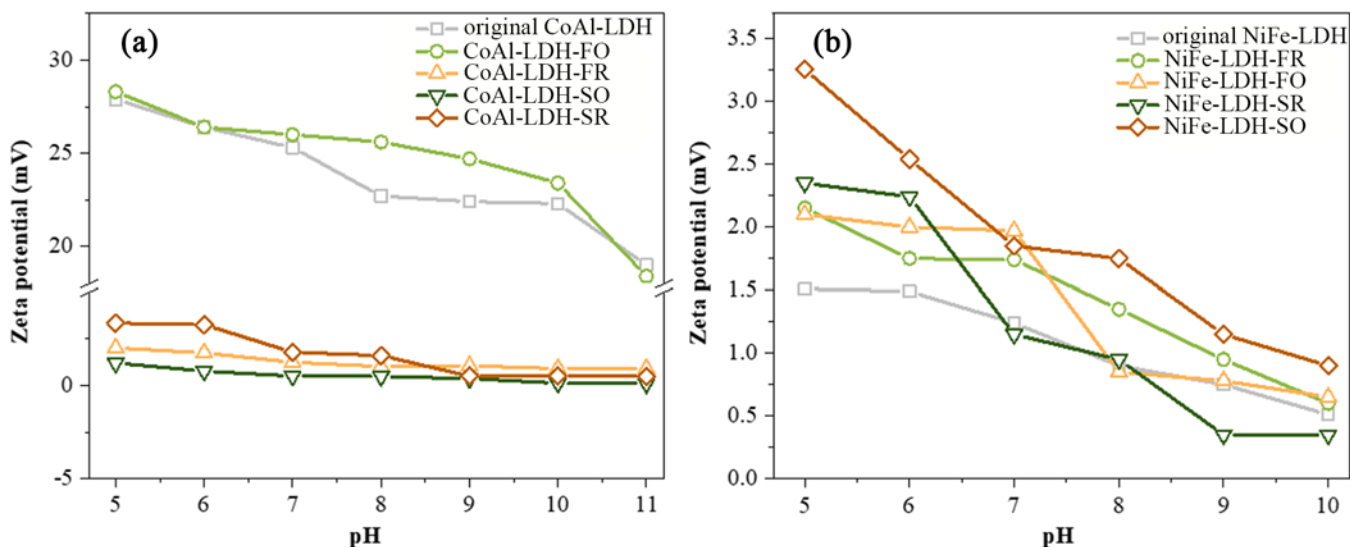


**Figure 2.** Variation of Zeta potential of the original, oxidised, and reduced LDH: (a) CoAl-LDH and its oxidised and reduced products; (b) NiFe-LDH and its oxidised and reduced products.

evolution showed little effect on the flake morphology, indicating that the structure of the LDH was not obviously affected, also in good agreement with XRD results. In summary, compared to CoAl-LDH, the structure of NiFe-LDH is more stable, and the oxidative–reductive process did not cause significant damage to its structure.

#### **Impact of redox evolution on the transfer and occurrence of heavy metals**

Each redox evolution caused 24.4%–93.5% of Co or Fe in CoAl-LDH and NiFe-LDH to be reduced or oxidised (Table 1), which suggested CoAl-LDH and NiFe-LDH could be partially reduced or oxidised. Leaching results of heavy metals indicates that ca. 2–3% of Co and Ni would transfer from the LDH structure

to solution after all the oxidation–reduction alternating processes (Fig. 4). Each oxidation or reduction resulted in the dissolution of heavy metals, and the oxidation process contributed to the transfer of heavy metals more significantly than the reduction process (0.8–1.3% for each oxidation process and 0.06–0.16% for each reduction process). The redox evolution also greatly affected the occurrence forms of heavy metal ions. The percentages of exchangeable, carbonate-bounded, and residual forms of metal elements in the original LDH and their oxidative–reductive evolution products were determined through leaching experiments (Fig. 5). The results indicated that the contents of exchangeable and carbonate-bounded forms of the metals are relatively low, while the content of the residual state is high, indicating that both LDHs have a strong ability to lock heavy metal ions. For original CoAl-LDH, the content of exchangeable (5.48%) and carbonate-bounded Co (46.30%) indicated that a half of Co did not enter the LDH structure. The low proportion of

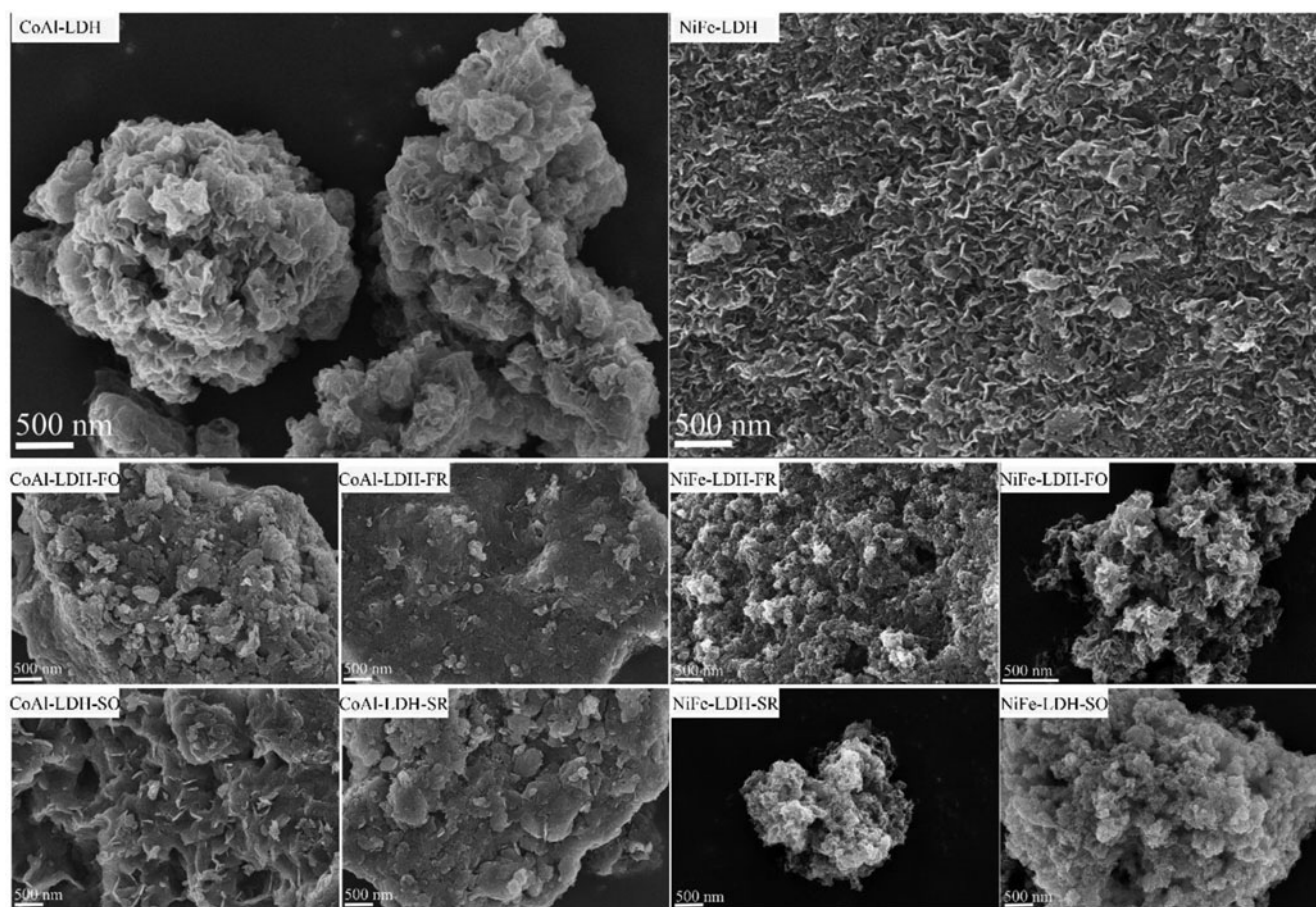


**Figure 3.** Variation of morphology of the original, oxidised, and reduced CoAl-LDH and NiFe-LDH.

**Table 1.** Redox ratio of Co and Fe in each redox reaction

| Sample      | Total Co or Fe (mg/g) | Co(II) or Fe(II) (mg/g) | Co(III) or Fe(III) (mg/g) | Co(II)/Co(III) or Fe(II)/Fe(III) | Redox ratio (%) |
|-------------|-----------------------|-------------------------|---------------------------|----------------------------------|-----------------|
| Co          |                       |                         |                           |                                  |                 |
| CoAl-LDH    | 370.7                 | 368.3                   | 2.4                       | 153.5                            | –               |
| CoAl-LDH-FO | 367.0                 | 277.5                   | 89.5                      | 3.1                              | 24.4            |
| CoAl-LDH-FR | 366.6                 | 360.8                   | 5.8                       | 62.2                             | 93.5            |
| CoAl-LDH-SO | 361.5                 | 205.7                   | 155.8                     | 1.3                              | 43.0            |
| CoAl-LDH-SR | 360.9                 | 338.1                   | 22.8                      | 14.8                             | 85.4            |
| Fe          |                       |                         |                           |                                  |                 |
| NiFe-LDH    | 174.8                 | 0.0                     | 174.8                     | 0.0                              | –               |
| NiFe-LDH-FR | 171.3                 | 64.8                    | 106.5                     | 0.6                              | 37.1            |
| NiFe-LDH-FO | 171.2                 | 11.5                    | 159.7                     | 0.1                              | 82.3            |
| NiFe-LDH-SR | 166.7                 | 92.3                    | 74.4                      | 1.2                              | 53.4            |
| NiFe-LDH-SO | 166.8                 | 7.4                     | 159.4                     | 0.0                              | 92.0            |

residual Al (66.11%) and high carbonate-bounded Al (33.89%) also suggested a third of the Al was not involved in the formation of CoAl-LDH. These results indicated that the original CoAl-LDH is a mixture of metal carbonate and LDHs. It can be seen that after multiple cycles of oxidative–reductive evolution, the carbonate-bounded Co and Al significantly transformed into the residual state (increased from 66.11% to 99.05% for Al, and 48.22% to 87.22% for Co), indicating that redox evolution contributed to a more stable state of heavy metal. This result demonstrated that the redox evolution of CoAl-LDH would result

in a more secure fixation of Co and a significant reduction in its bioavailability.

Regarding NiFe-LDH, redox evolution caused a gradual decrease of carbonate-bounded Fe (from 3.91% to 0), and a slight increase of residual form of Fe (from 96.09% to 99.50%, Fig. 5c). Meanwhile, redox evolution led to a decrease of exchangeable Ni (from 4.53% to 1.85%) and a slight increase of residual form of Ni (from 79.51% to 87.63%, Fig. 5d). But reduction would result in the increase of carbonate-bounded Ni (from 15.96% to 24.82%), whereas oxidation caused a contrary tendency. Overall,

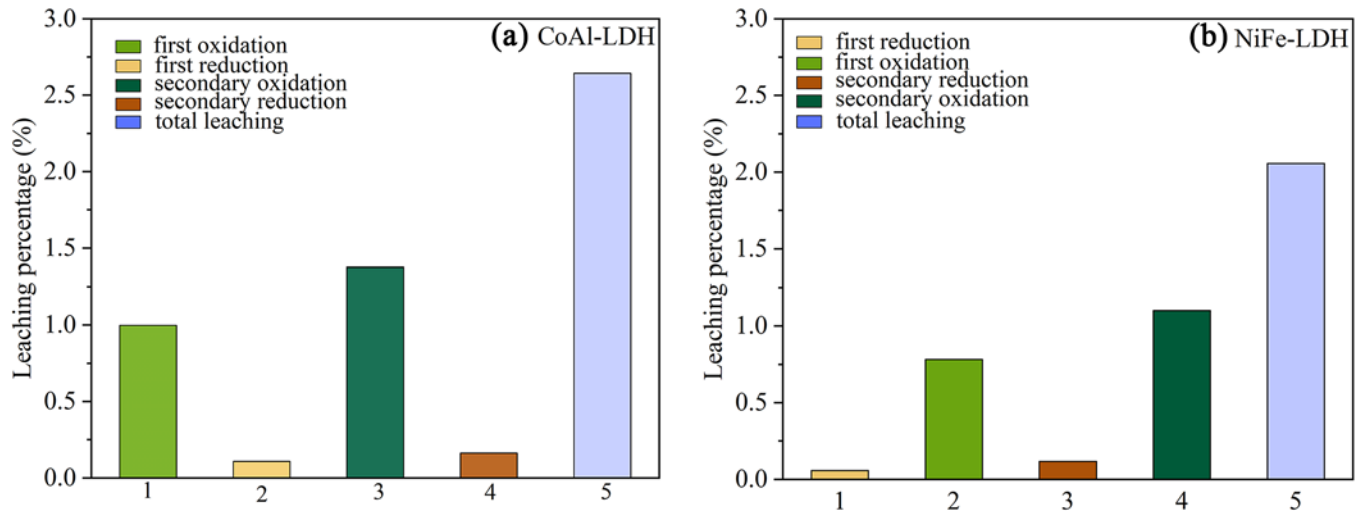


**Figure 4.** Leaching percentage of heavy metals during oxidation-reduction alternating evolution process: (a) leaching of Co in CoAl-LDH; (b) leaching of Ni in NiFe-LDH. Co content in the original CoAl-LDH is 370.7 mg/g LDH; Ni content in the original NiFe-LDH is 345.2 mg/g LDH.

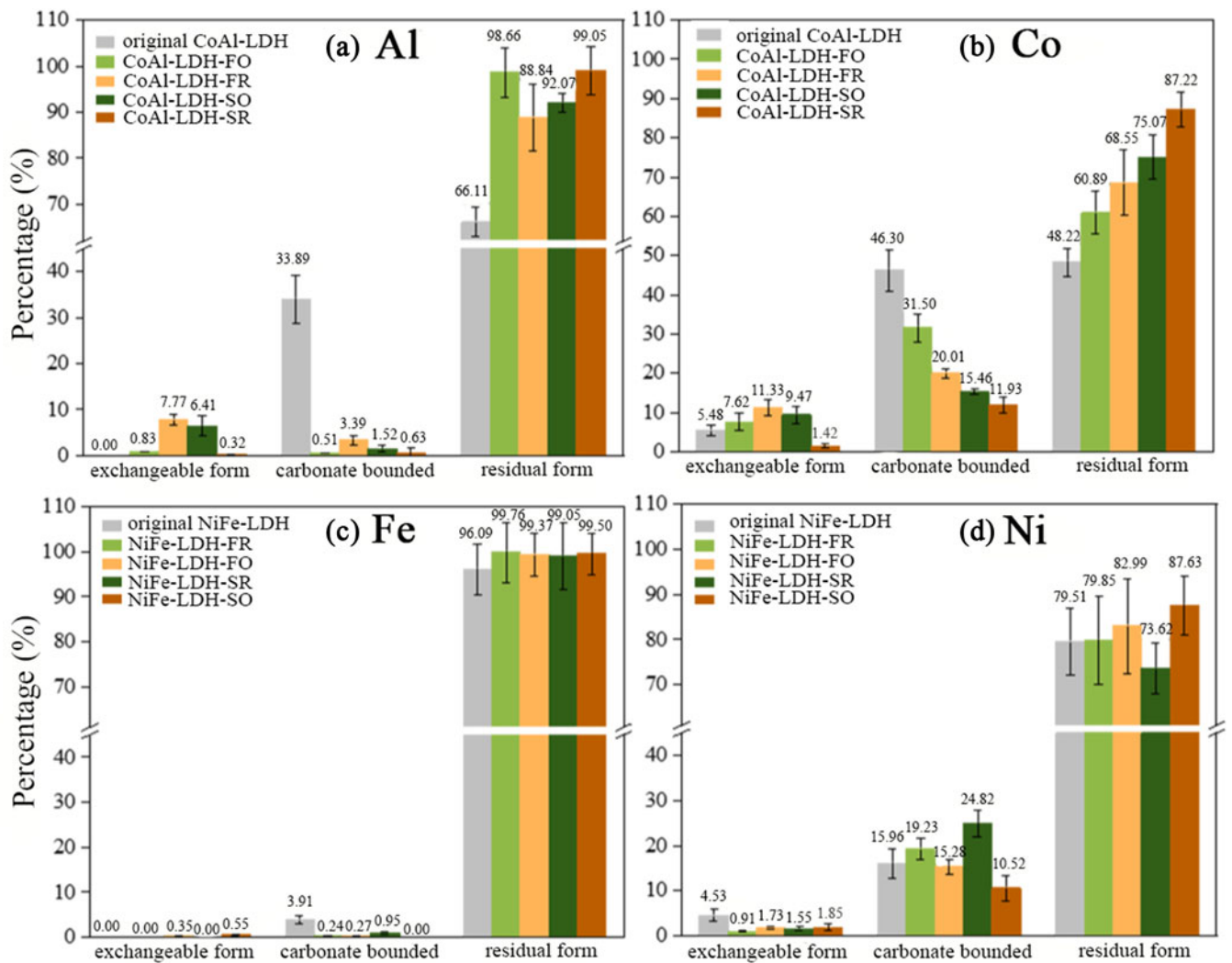


**Figure 5.** The occurrence of forms of Al, Co, Fe and Ni in the original, oxidised and reduced LDH: (a) Al in CoAl-LDH; (b) Co in CoAl-LDH; (c) Fe in NiFe-LDH; (d) Ni in NiFe-LDH.

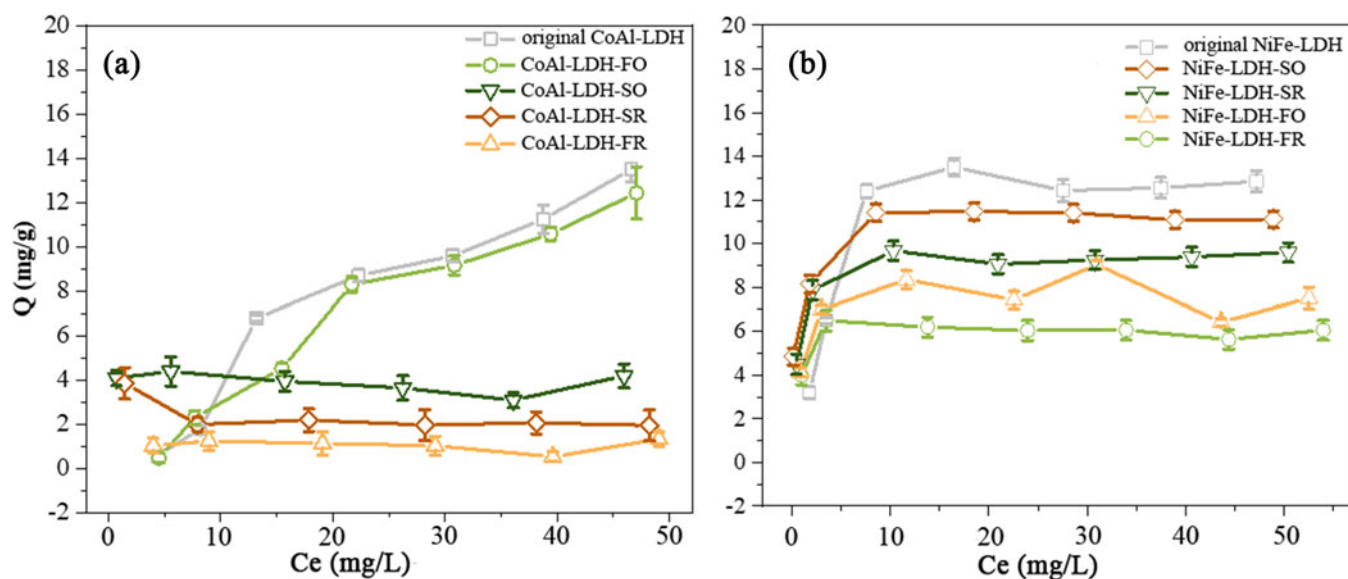


**Figure 6.** Variation of adsorptive performance to Cd(II) of the CoAl-LDH and NiFe-LDH after oxidation-reduction alternating evolution: (a) CoAl-LDH and its oxidised and reduced products; (b) NiFe-LDH and its oxidised and reduced products.

redox evolution can also result in a more secure fixation of Ni and a reduction in its bioavailability.

Combining the above results, it can be concluded that redox evolution leads to a tighter binding of heavy metal ions with the LDH structure or solid phase, resulting in a decrease in the content of bioavailable heavy metals. But it will also cause a small amount of heavy metal to transfer from a solid phase to a liquid phase during the redox process.

#### Impact of redox evolution on the adsorptive ability of LDHs

The redox evolution of the LDH affected not only the locking performance of heavy metal ions in their structure but also their adsorption ability for fixing heavy metal ions. The Cd(II) adsorption isotherms of CoAl-LDH, NiFe-LDH, and their oxidised and reduced products indicated that the redox evolution significantly decreased the adsorption capacity of the LDH (Fig. 6). For the original CoAl-LDH and its first oxidation product, they showed comparable adsorption performance to Cd(II) with maximum adsorption capacities of ca. 14 and 12 mg/g. This result should be due to their similar LDH structure, morphology, and zeta potential in pH 7 (Figs 1–3). The subsequent oxidative or reductive evolution strongly weakened the adsorption ability of the LDH (decrease from ca. 14 to 1 mg/g of the maximum adsorption capacity, Fig. 6a), which should be resulting mainly from the destruction of the LDH structure and formation of a denser aggregation of sheets and dense blocks (Figs 1 and 3). Similar results were observed for NiFe-LDH. The original NiFe-LDH exhibited the best adsorption performance for Cd(II), and the subsequent oxidative-reductive evolution greatly reduced the adsorption performance (decrease from c.a. 13 to 6 mg/g of the maximum adsorption capacity, Fig. 6b). The combination of variation of layered structure and decrease of zeta potential may be the main reason for the decrease of adsorptive ability (Figs 1 and 2). Considering the above experimental results, it can be concluded that the oxidative-reductive evolution is not conducive to LDHs exerting a fixation effect on surrounding heavy metal ions.

#### The relationship between the variation of structure characteristics and the fixation performance of heavy metals

As mentioned earlier, for CoAl-LDH, the alternating oxidative-reductive evolution caused the disappearance of all characteristic diffraction peaks belonging to LDHs after multiple oxidation and reduction cycles, the positive charge content of the structure significantly decreases (from 20–27 mV to 0–5 mV), and the sheet-like morphology of the LDH was remarkably destroyed. These results indicated that the oxidative-reductive evolution led to significant structural damage to CoAl-LDH. The structural damage resulted in a significant change in the occurrence form of heavy metal cobalt ions in the structure. In detail, the structural damage caused some cobalt ions to transform into an exchangeable form, and with the progression of the oxidative-reductive evolution, the exchangeable content gradually increased, suggesting an increase in the most bioavailable form. However, from Fig. 5b, it can be seen that the exchangeable cobalt mainly comes from the transformation of the carbonate-bounded state. At the same time, after the oxidative-reductive evolution, most of the carbonate-bounded state transformed into the residual state. Overall, the content of bioavailable heavy metals (exchangeable and carbonate-bounded states) gradually decreases with the progression of the oxidative-reductive evolution. However, considering the evolution of the CoAl-LDH structure, the increase in the content of residual state heavy metals is positively correlated with the structural damage of the LDH, indicating that the increase in the residual state may be due to the formation of cobalt oxides and/or hydroxides. Additionally, the evolution (damage) of the structure significantly reduced the purification ability of CoAl-LDH for surrounding heavy metal ions. The adsorption activity of a LDH for heavy metal ions mainly originates from structural hydroxyl groups, isomorphic substitution, and the availability of interlayer ions (Liang *et al.*, 2013, He *et al.*, 2018, Laipan *et al.*, 2023). The structural damage to the LDH would lead to a significant reduction in the content of structural hydroxyl groups, the number of octahedral vacancies in the LDH structure, and the content of interlayer anion active sites (Yang *et al.*, 2002). These are likely to be the reasons for the significant

decrease in the adsorption capacity for heavy metals of CoAl-LDH after redox evolution.

For NiFe-LDH, as analysed earlier, the oxidative–reductive evolution did not cause significant damage to the LDH structure; instead, it helped the growth of LDH crystals. The oxidative–reductive evolution to some extent sharpens the diffraction peaks belonging to LDHs (Fig. 1), and the structural charge increases (Fig. 2), indicating that the evolution contributed to the formation of the LDH structure. The improvement of LDH structure and increase of structure charge led to a decrease in the content of exchangeable heavy metals and an increase in the content of the residual state. In an open system, the formation and growth of a LDH can promote the conversion of carbon dioxide in the air into carbonate ions, which then enter the interlayers of a LDH as balancing anions (Laipan et al., 2018, Laipan et al., 2023). This may be the reason for the increase in the content of carbonate-bounded state heavy metals during evolution. This also reflects that the oxidative–reductive evolution contributes to the improvement of the NiFe-LDH structure. Similar to CoAl-LDH, the oxidative–reductive evolution helps to more securely lock the heavy metal ions in the LDH structure. However, the redox evolution also caused a decrease of the adsorptive ability of NiFe-LDH for surrounding heavy metals. The increase in surface positive charge may be an important reason for the decrease in its adsorption capacity. The electrostatic repulsion to some extent inhibits the contact of Cd(II) with the LDH surface. Overall, the fixation performance of LDHs for heavy metal ions in the structure and the surrounding environment is closely related to its structural evolution.

## Conclusion

This study investigated the influence of the change in metal oxidation states of the structural metal compositions of LDHs on the migration and transformation of structural and surface-adsorbed heavy metals, as well as the surface reactivity of LDHs towards surrounding heavy metals. The results indicated that the oxidative–reductive alternating evolution of LDHs constrained the transformation of heavy metals, as well as their bioavailability greatly. On the one hand, the alternating oxidative–reductive evolution helps LDHs to reduce the content of bioavailable heavy metals such as exchangeable and carbonate-bounded states, and makes the binding of heavy metal ions to LDHs more secure. The alternating oxidative–reductive evolution promoted the transformation of exchangeable and carbonate-bounded heavy metals into a residual state, reducing their mobility and bioavailability. Therefore, the alternating oxidative–reductive evolution enhanced the LDH's ability in the locking of its structural heavy metal ions. On the other hand, the oxidative–reductive evolution of the LDHs reduced their surface adsorption ability of surrounding heavy metals, thereby reducing their interfacial locking capacity for surrounding heavy metal ions. In the long run, this may reduce the environmental purification performance of LDHs for surrounding contaminants.

**Acknowledgements.** M. Laipan thanks the financial support from National Natural Science Foundation of China (41902039) and Natural Science Basic Research Program of Shaanxi Province (2024JC-YBQN-0319). J. Guo thanks the financial support from the Shaanxi Province Science and Technology Innovation Team (2022TD-09) and the Key Industrial Chain Project of Shaanxi Province (2022ZDLNY02-02).

**Author Contributions.** Mengyao Yuan performed the experiment and wrote the manuscript. Minwang Laipan conceived and designed the experiments, analysed the data, and edited the manuscript. Min Zhang, Xueya Wan, and

Ziyu Wang performed the characterisation section. Junkang Guo edited the manuscript.

**Conflicts of interest.** There are no conflicts to declare.

## References

- Ahmad N.N.R., Ang W.L., Teow Y.H., Mohammad A.W. and Hilal N. (2022) Nanofiltration membrane processes for water recycling, reuse and product recovery within various industries, A review. *Journal of Water Process Engineering*, **45**, 102478.
- Aucour A.-M., Bedell J.-P., Queyron M., Magnin V., Testemale D. and Sarret G. (2015) Dynamics of Zn in an urban wetland soil-plant system, Coupling isotopic and EXAFS approaches. *Geochimica et Cosmochimica Acta*, **160**, 55–69.
- de Souza E Silva P.T., de Mello N.T., Montenegro M.C., Araujo A.N., de Barros Neto B., and da Silva V.L. (2006) Extraction and recovery of chromium from electroplating sludge. *Journal of Hazardous Materials*, **128**, 39–43.
- Deng L., Zeng H., Shi Z., Zhang W. and Luo J. (2018) Sodium dodecyl sulfate intercalated and acrylamide anchored layered double hydroxides, A multifunctional adsorbent for highly efficient removal of Congo red. *Journal of Colloid Interface Science*, **521**, 172–182.
- Gou J., Xie S., Liu Y. and Liu C. (2016) Flower-like nickel-cobalt hydroxides converted from phosphites for high rate performance hybrid supercapacitor electrode materials. *Electrochimica Acta*, **210**, 915–924.
- Guo J., Zhao J., Ren X., Jia H., Muhammad H., Lv X., Wei T., and Hua L. (2020) Effects of Burkholderia sp., D54 on growth and cadmium uptake of tomato, ryegrass and soybean plants. *International Journal of Environmental Science Technology*, **17**, 1149–1158.
- Guo J., Wang L., Tu Y., Muhammad H., Fan X., Cao G. and Laipan M. (2021) Polypyrrole modified bentonite nanocomposite and its application in high-efficiency removal of Cr (VI). *Journal of Environmental Chemical Engineering*, **9**, 106631.
- Haris M., Hamid Y., Wang L., Wang M., Yashir N., Su F., Saleem A., Guo J. and Li Y. (2022) Cd diminution through microbial mediated degraded lignocellulose maize straw, Batch adsorption and bioavailability trails. *Journal of Environmental Management*, **302**, 114042.
- He X., Qiu X., Hu C. and Liu Y. (2018) Treatment of heavy metal ions in wastewater using layered double hydroxides, A review. *Journal of Dispersion Science and Technology*, **39**, 792–801.
- Laipan M., Fu H., Zhu R., Sun L., Steel R. M., Ye S., Zhu J. and He H. (2018) Calcined Mg/Al-LDH for acidic wastewater treatment, Simultaneous neutralization and contaminant removal. *Applied Clay Science*, **153**, 46–53.
- Laipan M., Yu J., Zhu R., Zhu J., Smith A.T., He H., O'Hare D. and Sun L. (2020) Functionalized layered double hydroxides for innovative applications. *Materials Horizons*, **7**, 715–745.
- Laipan M., Chen Q., Wang Z., Zhang M., Yuan M., Zhu R. and Sun L. (2023) Interlayer anions of layered double hydroxides as mobile active sites to improve the adsorptive performance toward Cd<sup>2+</sup>. *Inorganic Chemistry*, **62**, 13857–13866.
- Laipan M., Zhang M., Wang Z., Zhu R. and Sun L. (2024) Highly efficient recovery of Zn<sup>2+</sup>/Cu<sup>2+</sup> from water by using hydrotalcite as crystal seeds. *The Science of The Total Environment*, **914**, 169954–169954.
- Liang X., Zang Y., Xu Y., Tan X., Hou W., Wang L. and Sun Y. (2013) Sorption of metal cations on layered double hydroxides. *Colloids and Surfaces A, Physicochemical and Engineering Aspects*, **433**, 122–131.
- Liang X., Li Y., Wei G., He H., Stucki J.W., Ma L., Pentrakova L., Pentrak M. and Zhu J. (2019) Heterogeneous reduction of 2-chloronitrobenzene by co-substituted magnetite coupled with aqueous Fe<sup>2+</sup>, Performance, factors, and mechanism. *ACS Earth and Space Chemistry*, **3**, 728–737.
- Liu Q., Wang H., Wang X., Tong R., Zhou X., Peng X., Wang H., Tao H. and Zhang Z. (2017) Bifunctional Ni<sub>1-x</sub>Fe<sub>x</sub> layered double hydroxides/Ni foam electrodes for high-efficient overall water splitting, a study on compositional tuning and valence state evolution. *International Journal of Hydrogen Energy*, **42**, 5560–5568.
- Liu J., Zhu R.L., Xu T.Y., Laipan M.W., Zhu Y.P., Zhou Q., Zhu J.X. and He H.P. (2018) Interaction of polyhydroxy fullerenes with ferrihydrite, adsorption and aggregation. *Journal of Environmental Sciences*, **64**, 1–9.



- Liu Z., Xu Z., Xu L., Buyong F., Chay T.C., Li Z., Cai Y., Hu B., Zhu Y. and Wang X. (2022) Modified biochar, synthesis and mechanism for removal of environmental heavy metals. *Carbon Research*, **1**, 8.
- Liu X., Laipan M., Zhang C., Zhang M., Wang Z., Yuan M. and Guo J. (2024) Microbial weathering of montmorillonite and its implication for Cd (II) immobilization. *Chemosphere*, **349**, 140850.
- Muhammad H., Wei T., Cao G., Yu S., Ren X., Jia H., Saleem A., Hua L., Guo J. and Li Y. (2021) Study of soil microorganisms modified wheat straw and biochar for reducing cadmium leaching potential and bioavailability. *Chemosphere*, **273**, 129644.
- Peltier E., van der Lelie D. and Sparks D.L. (2010) Formation and Stability of Ni-Al Hydroxide Phases in Soils. *Environmental Science & Technology*, **44**, 302–308.
- Qiu M., Liu L., Ling Q., Cai Y., Yu S., Wang S., Fu D., Hu B. and Wang X. (2022) Biochar for the removal of contaminants from soil and water, a review. *Biochar*, **4**, 19.
- Siebecker M.G., Li W. and Sparks D.L. (2018) The important role of layered double hydroxides in soil chemical processes and remediation, what we have learned over the past 20 years. *Advances in Agronomy*, **147**, 1–59.
- Sodango T.H., Li X., Sha J. and Bao Z. (2018) Review of the spatial distribution, source and extent of heavy metal pollution of soil in China, impacts and mitigation approaches. *Journal of Health Pollution*, **8**, 53–70.
- Tessier A., Campbell P.G. and Bisson M. (1979) Sequential extraction procedure for the speciation of particulate trace metals. *Analytical Chemistry*, **51**, 844–851.
- Wang B., Liu F., Zhang F., Tan M., Jiang H., Liu Y. and Zhang Y. (2022a) Efficient separation and recovery of cobalt(II) and lithium(I) from spent lithium ion batteries(LIBs) by polymer inclusion membrane electrodialysis(PIMED). *Chemical Engineering Journal*, **430**, 132924.
- Wang L., Wang M., Muhammad H., Sun Y., Guo J. and Laipan M. (2022b) Polypyrrole-Bentonite composite as a highly efficient and low cost anionic adsorbent for removing hexavalent molybdenum from wastewater. *Journal of Colloid Interface Science*, **615**, 797–806.
- Xu M., Ma J., Zhang X.-H., Yang G., Long L.-L., Chen C., Song C., Wu J., Gao P. and Guan D.-X. (2023) Biochar-bacteria partnership based on microbially induced calcite precipitation improves Cd immobilization and soil function. *Biochar*, **5**, 20.
- Yang W., Kim Y., Liu P.K., Sahimi M. and Tsotsis T.T. (2002) A study by in situ techniques of the thermal evolution of the structure of a Mg–Al–CO<sub>3</sub> layered double hydroxide. *Chemical Engineering Science*, **57**, 2945–2953.
- Yu J., Wang Q., O'Hare D. and Sun L. (2017) Preparation of two dimensional layered double hydroxide nanosheets and their applications. *Chemical Society Reviews*, **46**, 5950–5974.
- Yu T., Zhou W., Zhang Y., Fang Y. and Cheng Y.J.S. (2024) Molecular dynamics simulation study on the interaction mechanisms of leaching solutions and LiCoO<sub>2</sub> surface. *Separation and Purification Technology*, **339**, 126596.
- Zhang Y., Haris M., Zhang L., Zhang C., Wei T., Li X., Niu Y., Li Y., Guo J. and Li X. (2022) Amino-modified chitosan/gold tailings composite for selective and highly efficient removal of lead and cadmium from wastewater. *Chemosphere*, **308**, 136086.
- Zhao Y., Wang Q., Bian T., Yu H., Fan H., Zhou C., Wu L.-Z., Tung C.-H., O'Hare D. and Zhang T. (2015) Ni 3+ doped monolayer layered double hydroxide nanosheets as efficient electrodes for supercapacitors. *Nanoscale*, **7**, 7168–7173.
- Zhou J.Z., Wu Y.Y., Liu C., Orpe A., Liu Q., Xu Z.P., Qian G.R. and Qiao S.Z. (2010) Effective self-purification of polynary metal electroplating wastewaters through formation of Layered Double Hydroxides. *Environmental Science & Technology*, **44**, 8884–8890.
- Zhu Y. and Elzinga E.J. (2014) Formation of layered Fe(II)-hydroxides during Fe(II) sorption onto clay and metal-oxide substrates. *Environmental Science & Technology*, **48**, 4937–4945.
- Zhu R., Chen Q., Zhou Q., Xi Y., Zhu J. and He H. (2016) Adsorbents based on montmorillonite for contaminant removal from water, A review. *Applied Clay Science*, **123**, 239–258.